Bistability of cell adhesion in shear flow

Artem Efremov and Jianshu Cao

Supporting Material

1. Force balance: the total tension of bonds in the rupture area.

The total tension Q_{tot} is determined by the load F and torque M created by the blood flow. In the simplest case when a rolling cell has approximately the shape of a sphere (with the radius r), the load F and torque M can be found using the following equations (1, 2):

$$\begin{cases} F \approx 6\pi\eta r\left[1.7rS + \left(0.4\ln\left(\delta / r\right) - 1.2\right)v\right] \\ M \approx 8\pi\eta r^2\left[0.5rS + \left(0.3\ln\left(\delta / r\right) - 0.6\right)v\right] \end{cases} \quad \text{(A1)}$$

Here S is the flow shear rate; δ ($\delta << r$) is the size of the gap between the rolling cell and the wall (see Fig. 1); η is the blood viscosity. To derive eq.A1, we assumed that the average velocity of the cell during steady-state rolling is $v = r\omega$ (here ω is the cell angular velocity), as was shown (3). I.e. there is no slip between the rolling cell and the wall, because adhesion bonds in the contact area restrict the motion of the cell membrane relative to the wall. To express the total tension Q_{tot} through the load F and torque M, one needs to solve mechanical equilibrium equations similar to those in ref. (4):

$$\begin{cases} M = rQ_{tot}\sin\beta \\ F = Q_{tot}\cos\left(\alpha + \beta\right) \\ P = Q_{tot}\sin\left(\alpha + \beta\right) \end{cases} \quad \text{(A2)}$$

Here P is the normal reaction force acting on the rolling cell, which is created by compressed bonds in the contact area excluding the rupture area; α and β are angles shown on Fig. 1. Taking into account that $cos(\alpha) = a/2r$, it follows from eq.A2 that:

$$Q_{tot} = \frac{2r}{a}\sqrt{F^2 + \frac{M^2}{r^2} + 2F\frac{M}{r}\sqrt{1 - \frac{a^2}{4r^2}}} \approx \frac{2r}{a}\left(F + \frac{M}{r}\right) \quad \text{(A3)}$$

Approximate formula in the right part of eq.A3 has more than 95% precision for $a \le r$. Therefore, from eq.A1 and A3 it follows that:

$$Q_{tot} \approx 4\pi\eta\frac{r^2}{a}\left[7.1rS + \left(2.4\ln\left(\delta / r\right) - 6.0\right)v\right] \quad \text{(A4)}$$

2. Kinetics. Bond rupture.

As mentioned in the main text, in order to find out how the average life time of an adhesion site τ changes with the tension Q applied to it we adopted a simple kinetic scheme depicted on Fig. 3 with kinetic rates given by the Bell-Evans' model (eq. 10).

Parameters $x^{\#}$ (binding potential width) and k_{off} (unstressed rupture rate) in eq.10 for different adhesion proteins can be experimentally determined in AFM (atomic force microscopy) or BFP (biomembrane force probe) experiments. Their typical values are $x^{\#}$ = 0.13-1.2 nm and k_{off} = 0.000005-9 s^{-1} (see table T1). Interestingly, from this table it is easy to see that shear flow experiments give $x^{\#}$ approximately ten times smaller than AFM/BFP experiments. Such apparent small value of $x^{\#}$ may result from the single bond assumption, which is frequently used to process data from shear flow experiments. I.e. during the data processing it is frequently assumed that in shear flow experiments only rupture of a single bond is observed. But simultaneous rupture of several bonds also may take place in these experiments. As mentioned in ref. (5), apparent $x^{\#}$ for a multiply bonded system could be significantly less than the physical value of $x^{\#}$ for the underlying individual bonds. Thus, the single bond assumption may lead to highly underestimated values of $x^{\#}$. To avoid this

problem, in our model we used $x^{\#}$ of a single selectin bond rupture obtained in AFM/BFP experiments.

The value of the binding rate k_{on} can be estimated knowing the local concentration of proteins in adhesion sites. Taking into account that the typical length of adhesion proteins is 30-50 nm (6), simple estimations give the value of this concentration about ~ 10-30 μM. For the most protein-protein interactions the second order binding rate is ~ 10^5-10^8 $M^{-1}s^{-1}$ (7). Thus, the bond formation rate between two proteins in an adhesion site is ~ 1-3000 s^{-1}. It should be noted here that rates k_+ and k_{on} correspond to different kinetic processes. k_+ is the rate for the initial diffusive binding of two proteins/protein clusters. This rate corresponds to the process of first bond formation between two proteins/protein clusters. At the same time, rate k_{on} is related to the subsequent formation of additional bonds between the two clusters. This is a much faster process due to the cooperative effect caused by proteins clustering – unbounded proteins in the adhesion site find their binding partners much quicker since they do not need to diffuse over a large distance in search of them.

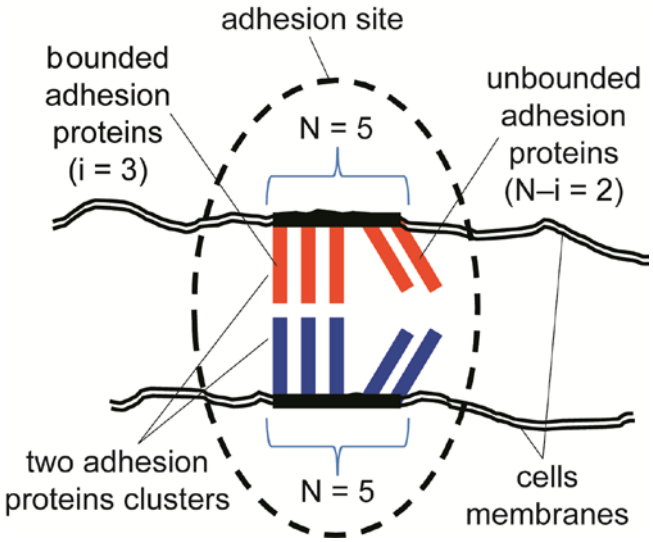

Figure S1. Schematic picture of a single adhesion site consisting from two protein clusters, $N = 5$.

The average lifetime of a single adhesion site can be obtained by calculating the mean turnover time (8, 9) for the chain reactions depicted on Fig.3:

$$\tau(N) = \sum_{i=1}^{N} \rho_i + \sum_{j=1}^{N-1} \left[\frac{1}{\rho_j k_{j,j+1}} \sum_{m=j+1}^{N} \rho_m \right] \qquad \text{(A5)}$$

Where:

$$\rho_1 = \frac{1}{k_{1,0}} \quad \text{and} \quad \rho_i = \prod_{j=1}^{i-1} k_{j,j+1} / \prod_{j=1}^{i} k_{j,j-1} \qquad \text{(A6)}$$

Exact eq. A5 for the average lifetime of an adhesion site can be further simplified for $N > 1$ by taking into account that typically $k_{on} >> k_{off}$. Thus, if the bonds tension Q is not very high, then $k_{i,i+1} >> k_{i+1,i}$, where $i = [1, N–1]$. Hence from eq. A5 it follows that the average lifetime of a single adhesion site under the tension Q can be approximated by the following formula:

$$\tau(N) \approx \rho_N = \frac{1}{k_{off}} \frac{(N-1)!}{N} \left(\frac{k_{on}}{k_{off}} \right)^{N-1} e^{-Qx^{\#} \sum_{i=1}^{N} i^{-1} / k_B T} \qquad \text{(A7)}$$

Eq. A7 is exact for $N = 1$ and gives reasonable values of the average adhesion site lifetime for $N > 1$ and tension $Q < k_BT/x^{\#} \times ln[k_{on}(N-1)^2/k_{off}]$. Eq. A7 agrees very well with the results acquired in ref.(10) – the average lifetime τ in the general case scales proportionally to $(k_{on}/k_{off})^{N-1}$.

3. Stability of the shear rate-velocity curve.

After finding all stationary solutions for a system, it is frequently necessary to establish their stability (11). In order to do that usually one should consider the sign of the variables time derivatives that govern the system changes. In our case using simple arguments, it is easy to show that a part of the stationary solution $S(v)$ that have a positive slope ($dS/dv > 0$) is a stable stationary solution branch, otherwise ($dS/dv < 0$) it is an unstable one.

To show that, let's first consider some point A on the curve $S(v)$ at which $dS/dv > 0$, see Fig. S2. To find out if this point is a stable one, we need to check how other points in its neighborhood (for example, points A_1 and A_2) behave with time (how the cell velocity changes) under the condition of a constant shear rate (frequent experimental condition). If these points move to the stationary point A, then it is stable one. Otherwise, if they go away from this point, it is unstable.

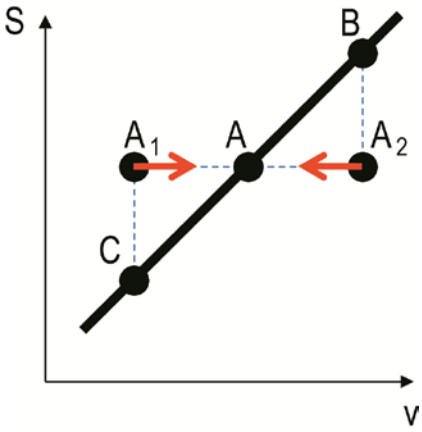

Figure S2. Example of a stable stationary solution branch.

For that purpose it is useful to consider the other two points (B and C) on the curve $S(v)$, see Fig.S2. Point A_1 is above point C. Therefore, to maintain the rolling velocity corresponding to point A_1 one needs the shear rate corresponding to point C which is smaller than one at point A_1. I.e. in other words at point A_1 the force created by the flow pushing the rolling cell is greater than the dynamic strength of the adhesion bonds. That means that a rolling cell starting from point A_1 has a positive acceleration and will increase its velocity until it reaches the velocity at point A. Quite similar arguments can be used for point A_2. It is located below point B. Hence, to maintain the rolling cell velocity corresponding to point A_2, one needs the shear rate corresponding to point B which is higher than one at point A_1. I.e. at point A_2 the flow force pushing the rolling cell is smaller than the dynamic strength of the adhesion bonds. That means that a rolling cell starting from point A_2 will decrease its velocity until it coincides with the velocity at point A. Thus, we can conclude that point A is, indeed, a stable one. Since this is true for any point at which $dS/dv > 0$ then the whole branch of the stationary solution curve $S(v)$ with a positive slope is a stable stationary solution.

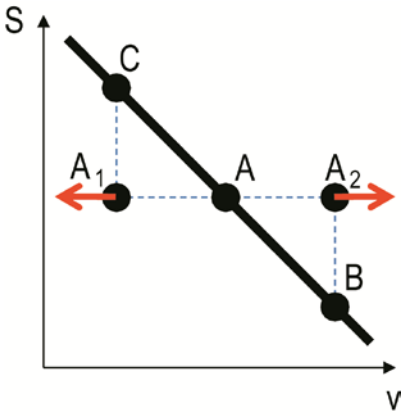

Figure S3. Example of an unstable stationary solution branch.

Similarly, it is easy to show that if the curve $S(v)$ has a negative slope ($dS/dv < 0$, see Fig. S3) at point A, then it is an unstable point. As can be seen from Fig. S3, this time point A_1 is below point C. I.e. the flow pushing force is weaker than the dynamic strength of the adhesion bonds. Hence, a rolling cell starting from point A_1 will decelerate (move away point A). At point A_2 the situation is opposite – dynamic strength of the adhesion bonds is not high enough to resist the flow pushing force and a rolling cell starting at point A_2 will accelerate (and again move away from point A). Therefore, since this is true for any point at which $dS/dv < 0$, the whole branch of the stationary solution curve $S(v)$ with a negative slope is an unstable stationary solution.

4. Physical origin of the adhesion bistability.

To better understand the physical origin of the adhesion bistability, let's consider two regimes of the cell movement: 1) at low velocities ($v << k_+a\sigma_0$) and 2) at high velocities ($v >> k_+a\sigma_0$). In the first case the surface concentration σ of adhesion sites on the trailing edge of the contact area is approximately described by the following equation, which is derived from eq. 6:

$$\sigma = \frac{k_+ a\sigma_0^2}{v + k_+ a\sigma_0} \approx \sigma_0 \qquad \text{(A8)}$$

Thus, at small velocities the surface concentration of adhesion sites at the trailing edge is at saturation. Given σ, one can obtain the following expression for the number of bonds which cells moving at velocity v must rupture per unit of time:

$$\frac{\Delta M}{\Delta t} = \sigma b v \qquad \text{(A9)}$$

For small velocities approximation from eq. A8 it follows that $\Delta M/\Delta t \approx \sigma_0 b v$, i.e. the number of ruptured bonds per unit of time is proportional to the cell velocity v. In contrast, for high velocities:

$$\sigma = \frac{k_+ a\sigma_0^2}{v + k_+ a\sigma_0} \approx \frac{k_+ a\sigma_0^2}{v} \qquad \text{(A10)}$$

Therefore, $\Delta M/\Delta t \approx k_+ ab\sigma_0^2$, i.e. the number of ruptured bonds per unit of time is velocity independent. Hence, at small velocities the shear rate-velocity curve $S(v)$ is mostly determined by the bond rupture process – the higher the cell velocity the more bonds must be ruptured per unit of time. Whereas at high velocities the number of bonds ruptured per unit of time is fairly constant and the curve behavior is mostly governed by purely hydrodynamic effects including viscous friction between the cell and the wall (the right term in eq. 12). Transition between these two rolling regimes is determined by the bond formation process

($k_+a\sigma_0$). Thus, the shape of the $S(v)$ curve and adhesion bistability results from the competition between the bond rupture and formation processes.

It is easy to obtain a linear approximation of the $S(v)$ curve for the regime of small velocities. For typical experimentally measured values of the model parameters the right term in eq. 12 gives very small contribution to the whole expression. Thus, it can be neglected under the small velocities approximation, and the $S(v)$ curve linear approximation at small velocities is given by the following expression:

$$S(v_0+\Delta v)\approx \frac{abc\sigma_0 k_B T}{28\pi\eta r^3 x^{\#}\left(1+v_0/k_+a\sigma_0\right)\sum_{i=1}^{N} i^{-1}}\frac{\Delta v}{v_0} \qquad \text{(A11)}$$

Here $\Delta v << v_0$, and velocity v_0 (at which the logarithm in eq. 12 equals to zero) is given by the following equation:

$$v_0 = ck_{off}\frac{N}{(N-1)!}\left(\frac{k_{off}}{k_{on}}\right)^{N-1} \qquad \text{(A12)}$$

The small velocities linear approximation at two different scales is shown on Fig. S4.

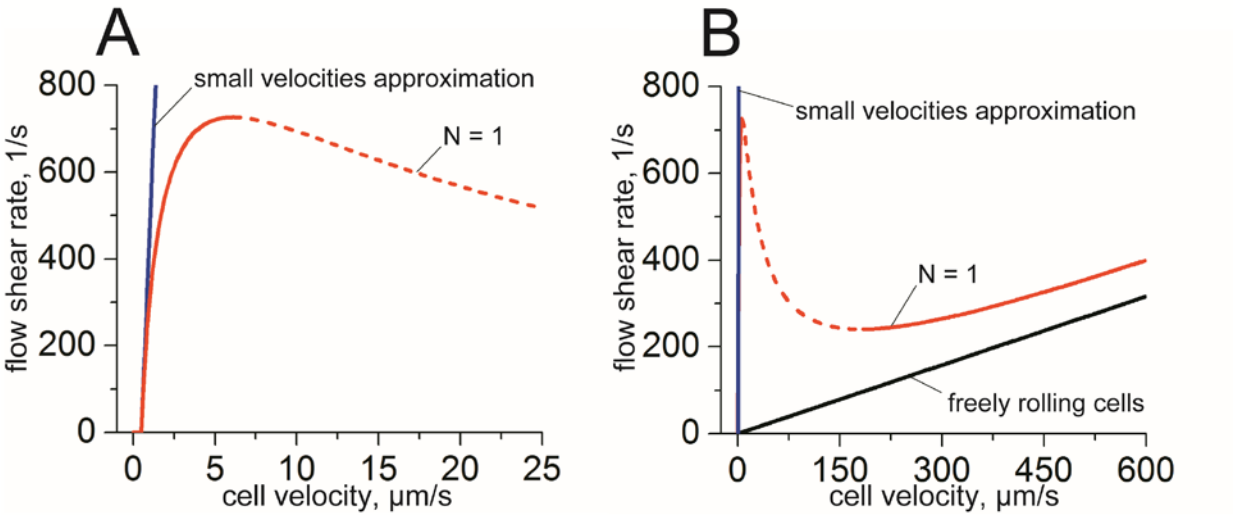

Fig. S4, A and B. Linear approximation of the $S(v)$ curve at small velocities. The red curve corresponds to rolling cells, which have bonds with the wall. The black line corresponds to freely rolling cells, which do not have bonds with the wall. Values of the model parameters used in calculations for panels A and B are shown in table 1.

Table T1. Adhesion proteins rupture parameters.

Interaction	Method	$x^{\#}$, nm	k_0^{off}, s^{-1}	Reference
endothelium cells-E-selectin + granulocyte	shear flow	0.031	0.7	(12)
surface-E-selectin + neutrophil	shear flow	0.018	2.6	(13)
surface-E-selectin + surface-sLEx	fiber cantilever	0.034	0.82	(5)
surface-P-selectin + neutrophil	shear flow	0.04	0.93	(14)
transfected cells-P-selectin + CHO-cells-PSGL-1	shear flow	0.029	1.1	(15)
surface-P-selectin + neutrophil	shear flow	0.039	2.4	(13)
surface-PSGL-1 + neutrophil	BFP	0.24	1.2	(16)
surface-PSGL-1 + surface-P-selectin	BFP	0.23	0.45	(17)
surface-P-selectin + surface-PSGL-1	AFM	0.25	0.022	(18)
surface-P-selectin + neutrophil	AFM	0.13	0.2	(19)
surface-P-selectin + surface-G1	AFM	0.46	0.22	(20)
surface-L-selectin + neutrophil	shear flow	0.24	7	(21)
surface-L-selectin + neutrophil	shear flow	0.111	2.8	(13)
transfected cells-L-selectin + CHO-cells-PSGL-1	shear flow	0.16	8.6	(15)
surface-PNAd + neutrophil	shear flow	0.02	6.8	(12)
surface-PNAd + neutrophil	shear flow	0.059	3.8	(13)
surface-C-cadherin + surface-C-cadherin	BFP	0.78 0.78 0.98 1.04	3.93 0.019 0.00039 0.00001	(22)
surface-E-cadherin + surface-E-cadherin	BFP	0.63 0.63 0.82 1.2	9 0.7 0.01 0.000005	(23)

References.

1. Goldman, A. J., R. G. Cox, and H. Brenner. 1967. Slow viscous motion of a sphere parallel to a plane wall-I Motion through a quiescent fluid. Chem. Eng. Sci. 22:637-651.
2. Goldman, A. J., R. G. Cox, and H. Brenner. 1967. Slow viscous motion of a sphere parallel to a plane wall-II Couette flow. Chem. Eng. Sci. 22:653-660.
3. Hammer, D. A., and S. M. Apte. 1992. Simulation of cell rolling and adhesion on surfaces in shear flow: general results and analysis of selectin-mediated neutrophil adhesion. Biophys. J. 63:35-57.
4. Hammer, D. A., and D. A. Lauffenburger. 1987. A dynamical model for receptor-mediated cell adhesion to surfaces. Biophys. J. 52:475-487.
5. Tees, D. F. J., R. E. Waugh, and D. A. Hammer. 2001. A microcantilever device to assess the effect of force on the lifetime of selectin-carbohydrate bonds. Biophys. J. 80:668.
6. Springer, T. A. 1990. Adhesion receptors of the immune system. Nature 346:425-434.
7. Janin, J. 1995. Principles of protein-proteh recognition from structure to thermodynamics. Biochimie 77:497-505.
8. Bar-Haim, A., and J. Klafter. 1998. On mean residence and first passage times in finite one-dimensional systems. J. Chem. Phys. 109:5187-5193.
9. Cao, J., and R. J. Silbey. 2008. Generic schemes for single-molecule kinetics. 1: self-consistent pathway solutions for renewal processes. J. Phys. Chem. B 112:12867-12880.
10. Erdmann, T., and U. S. Schwarz. 2004. Stability of adhesion clusters under constant force. Phys. Rev. Lett. 92:108102.
11. Guckenheimer, J., and P. Holmes. 1983. Nonlinear oscillations, dynamical systems, and bifurcations of vector fields. Springer-Verlag, New York.
12. Alon, R., S. Chen, K. D. Puri, E. B. Finger, and T. A. Springer. 1997. The kinetics of L-selectin tethers and the mechanics of selectin-mediated rolling. J. Cell Biol. 138:1169-1180.
13. Smith, M. J., E. L. Berg, and M. B. Lawrence. 1999. A direct comparison of selectin-mediated transient, adhesive events using high temporal resolution. Biophys. J. 77:3371-3383.
14. Alon, R., D. A. Hammer, and T. A. Springer. 1995. Lifetime of the P-selectin-carbohydrate bond and its response to tensile force in hydrodynamic flow. Nature 374:539-542.
15. Ramachandran, V., M. U. Nollert, H. Qiu, W.-J. Liu, R. D. Cummings, C. Zhu, and R. P. McEver. 1999. Tyrosine replacement in P-selectin glycoprotein ligand-1 affects distinct kinetic and mechanical properties of bonds with P- and L-selectin. Proc. Natl. Acad. Sci. USA 96:13771-13776.
16. Evans, E., V. Heinrich, A. Leung, and K. Kinoshita. 2005. Nano- to microscale dynamics of P-selectin detachment from leukocyte interfaces. I. Membrane separation from the cytoskeleton. Biophys. J. 88:2288-2298.
17. Evans, E., A. Leung, V. Heinrich, and C. Zhu. 2004. Mechanical switching and coupling between two dissociation pathways in a P-selectin adhesion bond. Proc. Natl. Acad. Sci. USA 101:11281-11286.
18. Fritz, J., A. G. Katopodis, F. Kolbinger, and D. Anselmetti. 1998. Force-mediated kinetics of single P-selectin/ligand complexes observed by atomic force microscopy. Proc. Natl. Acad. Sci. USA 95:12283-12288.

19. Hanley, W., O. McCarty, S. Jadhav, Y. Tseng, D. Wirtz, and K. Konstantopoulos. 2003. Single molecule characterization of P-selectin/ligand binding. J. Biol. Chem. 278:10556-10561.
20. Marshall, B. T., M. Long, J. W. Piper, T. Yago, R. P. McEver, and C. Zhu. 2003. Direct observation of catch bonds involving cell-adhesion molecules. Nature 423:190-193.
21. Alon, R., S. Chen, R. Fuhlbrigge, K. D. Puri, and T. A. Springer. 1998. The kinetics and shear threshold of transient and rolling interactions of L-selectin with its ligand on leukocytes. Proc. Natl. Acad. Sci. USA 95:11631-11636.
22. Bayas, M. V., A. Leung, E. Evans, and D. Leckband. 2006. Lifetime measurements reveal kinetic differences between homophilic cadherin bonds. Biophys. J. 90:1385-1395.
23. Perret, E., A. Leung, H. Feracci, and E. Evans. 2004. Trans-bonded pairs of E-cadherin exhibit a remarkable hierarchy of mechanical strengths. Proc. Natl. Acad. Sci. USA 101:16472-16477.